Journal of Ceramic Processing Research. Vol. 25, No. 5, pp. 853~861 (2024)
(Received 4 July 2024, Received in revised form 27 July 2024, Accepted 11 September 2024)
https://doi.org/10.36410/jcpr.2024.25.5.853

J O U R N A L O F
Ceramic Processing Research

Gamma radiation effect on a murataite ceramic doped with Sr and Cs

Aicha Maachou[a,b,*], Salah Blizak[b,c], Nour El Hayet Kamel[#], Dalila Moudir[a], Badis Rahal[a], Ali Sari[d], Yasmina Mouheb[a] and Soumia Kamariz[a]

[a]*Nuclear Research Center of Algiers, 2 Boulevard Frantz Fanon, P.O. Box: 399, Alger-RP, 16000, Algiers, Algeria*
[b]*Research Unit for Materials, Processes and Environment URMPE, M'hamed Bougara University of Boumerdes, P.O. Box: 35000, Boumerdes, Algeria*
[c]*University of M'sila, University Pole, Road Bourdj Bou Arreiridj, M'sila 28000 Algeria*
[d]*Nuclear Reserch Center of Birine, P.O. Box: 17200, Ain Oussera, Algeria*
[#]*Retired from the Nuclear Research Center of Algiers, Co-supervisor of the Thesis, and Initiator of the Research Topic*

This study investigates the influence of gamma radiation, emitted by a Cobalt-60 source, on the structural modifications of a polysomatic ceramic of the Murataite type, intended for the containment of radioactive waste. The matrix is doped with Sr and Cs to simulate both radioactive alkaline and alkaline-earth isotopes. Samples are irradiated with a total dose of 10^5 Gy. After irradiation, the Archimedes density increases by 9.80% and 10.61% for undoped and Sr-doped ceramics, respectively. However, it decreases by 3.05% and 3.65% for Cs-doped ceramics and Sr-Cs co-doped ceramics, respectively. All measured values are below 4 g/cm^3. For all materials, the main XRD identified phase is 5M Murataite. After irradiation, this phase decreases significantly for both Cs and (Sr,Cs) doped materials, revealing that the particles movements under irradiation favours Cs and Sr-Cs hosting in the Zincohoegbomite secondary formed phase, which growth significantly after irradiation. The SEM observations reveal the crystalline grains morphological features, with few micrometers' sizes. The ceramics' Vickers microhardness is not affected and ranges between 410 and 646 HV. In conclusion, both the reference material and Sr-Mur material composition are the optimum chemical composition and give the optimum murataites' phase content after irradiation.

Keywords: Gamma-radiation, Murataite, Sintering, Characterizations.

Introduction

The research in the field of nuclear waste confinement ceramics is in progress. Since the simple crystalline structures are limitative in their isotopes loading rates, the complex structures become interesting as they offer the opportunity of confining a large variety of isotopes in their structure compared to that of simple crystalline phases. Moreover, they are characterized by a strong resistance against self-irradiation damages occurring in long-term waste disposal conditions [1]. Among these complex structures, the polysomatic ones are made of a flexible stack of structural crystalline units [2].

This investigation is focused on a polysomatic series, namely a Murataite polycrystalline structure. The Murataite minerals have the general formula of $^{VIII}A_6{}^{VI}B_{12}{}^{IV}C_4TX_{40}$ (A = Y, Na, Ca, REE, An; B = Ti, Fe, Al; C = Fe, Mn; T = Zn, Zr, Ce; X = O, F), where REE is a rare-earth element, and An an actinide element [3].

Many authors describe Murataite as an isometric derivative of the fluorite structure with the general formula $A_4B_2C_7O_{22-x}$ ($0 \leq x \leq 1$), where eight-coordinated A-sites are occupied by Na^+, Ca^{2+}, REE^{3+} or $An^{3+/4+}$ cations, four-and five-coordinated B-sites are filled with $Mn^{2+/3+}$, Zn^{2+} cations, and six coordinated C-sites are occupied by Ti^{4+}, Fe^{3+} or Al^{3+} cations [3-7].

Murataite structure is close to this of pyrochlore, which consist of a 2×2×2 fluorite unit cells' multiples. Pyrochlore and Murataite are expected to form polysomatic series.

Thus, Murataite occurs as multiples of three-(noted: 3C or 3M), five-(noted 5C or 5M), seven-(noted 7C or 7M), and eight-fold (noted 8C or 8M) fluorite unit cells. The structure of 5M, 7M and 8M phases consists of pyrochlore (two-fold elementary fluorite unit cell -2M) and Murataite (3M) units [4-9]. The whole of them has a cubic symmetry [10].

In a chemical point of view, the 3M fold Murataites formula consists of a ratio close to 27 cations for 42 O^{2-} anions; the 5M formula is in accordance with a ratio of 125 cations for 172 O^{2-} anions, and the 8M formula exhibit an elementary unit with a ratio of 486 cations to 823 O^{2-} anions.

Since the Murataites crystalline structures are complex,

*Corresponding author:
Tel : (213) 676 23 67 76
Fax: (213) 023 49 52 75
E-mail: a.maachou@crna.dz and a.maachou@univ-boumerdes.dz

their synthesis often leads to polyphasic phases' formation.

The synthesis of ceramics for the confinement of radioactive elements must meet many requirements. It should be safe, and the final products should have suitable physico-chemical, mechanical and durability properties. Thus, the materials should be well densified, with isotropic properties, and resistant against mechanical stresses.

Many synthesis routes can achieve this goal, such as the dry routes (metallurgical processes) as well as the wet processes (i.e. sol-gel) [11]. In both cases, the parameters affecting the final products' properties must be mastered.

Among the parameters affecting the materials densification during the solid-state synthesis, γ-rays irradiation creates lattice vacancies in the crystalline structures. It raises the diffusion coefficient of oxygen ions, and thus induces particles 'displacements, mainly traduced by an increase of ions' diffusion. The alkaline and alkaline-earth elements are more labile than the heavier elements, and are the first moved elements in the structure, affecting the lattice parameters and the contents of the crystals where they are present.

The particles displacements can induce thermal annealing of defects during the solid-state synthesis.

All these phenomena may affect the materials porosity, [12, 13] the phases' structure and chemical composition, and consequently resulting in the appearance of new phases along with some defects in the materials structure [14]. Adding to that, the crystalline phases' contents may change under gamma irradiation and, depending on the total radiation absorbed dose, in many cases; it is oriented such that the phases' percentage consequently varies [15].

All these phenomena are useful in many research areas. For example, the γ irradiations can improve the materials optical properties intended for laser applications purposes. Numerous studies report the effect of γ irradiation on the materials electrical properties (dielectric constant, dielectric loss, conductivity, supra-conductivity, etc.) directly in relation with cavity formations and blistering in the crystalline structures, [16, 17] and laser fibers performance (absorption, fluorescence, and luminescence' properties) [18, 19]. Also, γ irradiation improves the mechanical properties in both natural and synthetic fiber reinforcements, used in aeronautics, aerospace, civil engineering, automobile, etc. [6, 20, 21].

Adding to that, in the pharmaceutical field, both waters intended for injections and saline solutions are sterilized by gamma radiations. For products stability purposes, many antibiotics products and numerous drugs and products are also treated by gamma rays [22].

In this work, we report the γ-radiation effect on the physical and structural properties of a Murataite ceramic (noted Mur) intended for the confinement of radioactive waste, in which Mn has been replaced by Zn element [23]. This last is abundant in many radioactive wastes.

Zn may occupy the Mn element position in the crystalline structure without creating significant changes, due to their neighbouring atomic radii in the (+2) valence state ($r(Zn^{IV})$=0.60 Å, $r(Zn^{V})$=0.68 Å and $r(Mn^{IV})$=0.66 Å, $r(Mn^{V})$=0.75 Å) [24].

The polysomatic murataite structure is known for confining actinides/lanthanides elements. In the present study, 7% of Er simulate such elements, and 7% of Zr can be partially substituted by heavy atoms during the phases' formation process during synthesis.

And we focused on the influence of alkaline and alkaline earth elements as Sr and Cs, during the gamma irradiation of the confinement matrix. Different chemical compositions are synthesized by a dry route: the first doped with Sr (noted Sr-Mur), the second, with Cs (noted Cs-Mur) and the third with both elements (noted (Sr-Cs)-Mur).

A reference Murataite ceramic, free of Sr and Cs (noted Mur), is synthesized with the chemical composition (in wt.%) of: 10% ZnO, 12% CaO, 7% Er_2O_3, 53% TiO_2, 7% ZrO_2, 6% Fe_2O_3, 5% Al_2O_3. The microstructural characterizations (density, XRD, SEM, microhardness) are carried out before and after γ-radiation.

Experimental

Materials synthesis

Four Murataite ceramics: Mur, Sr-Mur, Cs-Mur, and (Sr-Cs)-Mur are synthesized by the metallurgical powder route method, according to the chemical compositions given in Table 1.

The following chemical reagents are employed: ZnO (Merck, 99%), CaO (Merck, 97%), SrO (Merck, 97%), Cs_2O (Biochim, 99.5%), Er_2O_3 (Fluka, 99,99%), TiO_2 (Merck, 99%), ZrO_2 (Aldrich, 99,99%), Fe_2O_3 (Merck, 99%), and Al_2O_3 (Aldrich, 99%).

The powders are grinded in a manual Agate mortar, and mixed according to the materials' stoichiometric chemical formula (Table 1). All doping elements are in their cold form and are chemical surrogates of the radionuclides wastes. Batches of 25 g of the mixed green materials are added with 4 wt.% of zinc stearates (Sigma-Aldrich), an organic binder. A Kernals balance is employed for weighing purposes ($\pm 10^{-4}$ g). The mixtures are homogenized during 6 h using an adapted D 403 Controls Automatic Sieve Shaker. Pellets with 17.2 mm diameters and variable heights are compacted using a Sodemi RD uni-axial press, at 400 MPa. They are sintered in a BLF-1800 Carbolite furnace at 1250 °C for 4 h, with a heating step of 5°/min and a natural cooling. After grinding, they are pelletized a second time in the same conditions and sintered again at 1250 °C for 10 h with the same heating cycle.

The samples are divided in two lots, the first one is lived without further treatment, and the second is irradiated at the Co-60 gamma radiation experimental

Table 1. Chemical composition of Murataites materials.

Ceramic	Chemical formula			
Mur	$Zn_{12.25}Ca_{21.38}Er_{4.02}Ti_{66.35}Zr_{5.67}Fe_{7.5}Al_{9.7}O_{83.55}$			
Sr-Mur	$Zn_{12.25}Ca_{12.47}Sr_{4.82}Er_{4.02}Ti_{66.35}Zr_{5.67}Fe_{7.5}Al_{9.78}O_{82.79}$			
Cs-Mur	$Zn_{12.24}Ca_{12.47}Cs_{3.54}Er_{4.02}Ti_{66.35}Zr_{5.67}Fe_{7.5}Al_{9.78}O_{78.58}$			
(Sr-Cs)-Mur	$Zn_{12.50}Ca_{12.47}Cs_{1.41}Sr_{1.92}Er_{4.02}Ti_{66.35}Zr_{5.67}Fe_{7.50}Al_{9.78}O_{80.21}$			
Oxides	Content (wt.%)			
ZnO	10	10	10	10
CaO	12	7	7	7
SrO	×	5	×	2
Cs_2O	×	×	5	3
Er_2O_3	7	7	7	7
TiO_2	53	53	53	53
ZrO_2	7	7	7	7
Fe_2O_3	6	6	6	6
Al_2O_3	5	5	5	5

facility of the Nuclear Research Center of Algiers. The samples are located at 10 cm from the γ-source. The total gamma dose is about 10^5 Gy, with a dose rate of 10.75 Gy/min. Both irradiated and non-irradiated sintered materials are characterized.

Materials characterization

The pellets densities (ρ_A), before and after irradiation, are measured by the Archimedes method using a Radwag AS 220-R2 hydrostatic balance at room temperature, with water as immersion liquid. The results are mean values of three repeated measures. The accuracy of the measurements is about ±0.001 g.

The XRD materials phases' identification is carried out using a PANalytical X'Pert Pro X-ray diffractometer with the wavelength of copper (λCu=1.54059 Å) with a step of 5°/min. The High Score Plus software is used for the spectra treatment [25]. The materials microscopic morphological properties are observed using a XL-30 ESEM FEG scanning electron microscope (SEM) in the BSE mode. The microhardness measurements are made with an Innovatest Falcon 400 Vickers indenter on polished pellets' surfaces, with a loading force ranging from 200 to 4000 gf. For each case, 10 measurements are made. The load corresponding to the less error is selected to estimate the Vickers microhardness; the results being the average of 10 measures. The materials microscopic morphological properties are observed using a XL-30 ESEM FEG scanning electron microscope (SEM) in the BSE mode. The microhardness measurements are made with an Innovatest Falcon 400 Vickers indenter on polished pellets' surfaces, with a loading force ranging from 200 to 4000 gf. For each case, 10 measurements are made. The load corresponding to the less error is selected to estimate the Vickers microhardness; the results being the average of 10 measures.

Results and Discussions

Materials densities

Both the measured and calculated materials densities are given in Table 2, and compared with values of the literature. The Archimedes density of the sintered materials increases slightly by doping Murataite with Cs (Cs-Mur) and co-doping it with Sr and Cs ((Sr-Cs)-Mur). This is due to the presence of Cs in the composition of the first two ceramics which has a high atomic mass (132.9054 amu), [26] compared to strontium element (87.62 amu) present in the two other ceramics.

After irradiation, the Archimedes densities increased

Table 2. Comparison between the Archimedes density ρ_A (g/cm^3) of the synthesized Murataites before and after γ-irradiation.

Chemical composition	Type	Density				Ref
		Geometrical	Theoretical	Archimedes		
		Unirradiated		irradiated		
Mur	5M	-	4.20	3.415	3.752	Us
Sr-Mur	5M	-	4.19	3.355	3.711	Us
Cs-Mur	5M	-	4.09	3.866	3.748	Us
(Sr-Cs)-Mur	5M	-	4.10	3.833	3.693	Us
$^{3.9\%}SrO$, $^{21.9\%}MoO_3$, $^{27.3\%}CeO_2$, $^{25.5\%}Pr_6O_{11}$, $^{5.0\%}Nd_2O_3$, $^{7.8\%}Sm_2O_3$, $^{5.3\%}Eu_2O_3$, $^{3.3\%}UO_2$	5M 3M	4.05	-	-	-	[21]
$Ca_{2.73}Mn_{2.16}Fe_{0.44}Ti_{14.28}Tb_{1.71}Al_{1.26}Zr_{1.71}O_{42}$	3M	-	4.568	-	-	[28]
$Al_{25.44}$ $Ca_{55.96}$ $Ti_{282.20}$ $Mn_{53.72}$ $Fe_{17.24}$ $Zr_{15.00}Ho_{36.6}$ O_{823}.	8M	-	4.541	-	-	[29]
$^{5.80\%}Na_2O$, $^{12.06\%}Y_2O_3$, $^{0.17\%}Gd_2O_3$, $^{2.18\%}Dy_2O_3$, $^{0.57\%}Ho_2O_3$, $^{3.09\%}Er_2O_3$, $^{0.34\%}Tm_2O_3$, $^{2.96\%}Yb_2O_3$, $^{0.34\%}Li_2O_3$, $^{0.90\%}CaO$, $^{0.11\%}PbO$, $^{0.17\%}SnO$, $^{0.61\%}MnO$, $^{12.45\%}ZnO$, $^{4.37\%}FeO$, $^{37.87\%}TiO_2$, $^{10.01\%}Nb_2O_5$, $^{6.55\%}F$, $^{0.55\%}H_2O$.	3M	-	4.64	4.69	-	[6]
$Ca_{2.5}Mn_2Th_{0.41}Cm_{0.12}Ti_{7.5}Zr_{0.5}AlFeO_{24.5}$.	5M	4.05	-	-	-	[27]
$Ca_{3.17}Mn_{1.39}U_{0.92}Zr_{0.79}Ti_{8.57}Fe_{0.30}Al_{0.34}O_{26.09}$	5M	-	4.98	-	-	[30]

by 9.80% and 10.61% for Mur and Sr-Mur ceramics, respectively. On the other hand, it decreases by 3.05% and 3.65% for the Cs-Mur and Sr-Cs-Mur ceramics, respectively. This shows that γ-radiation has a significant effect on the ceramics' Archimedes density. The gamma radiation influences the crystalline phases' contents, which have different densities, thus affecting the materials' global density. Adding to that, the irradiation may raise the porosity in the microstructure impacting the materials density, especially for Cs-Mur and Sr-Cs-Mur materials. A.A. Lizin et al. [21] have synthesized by sintering at 1350 °C a structure based on Murataite for the decontamination of glove boxes and hot cells' equipment. They report a geometrical density of 4.05 g/cm^3. This value is also found in the study carried out by A.N. Lukinykh et al. [27] which synthesized a Murataite

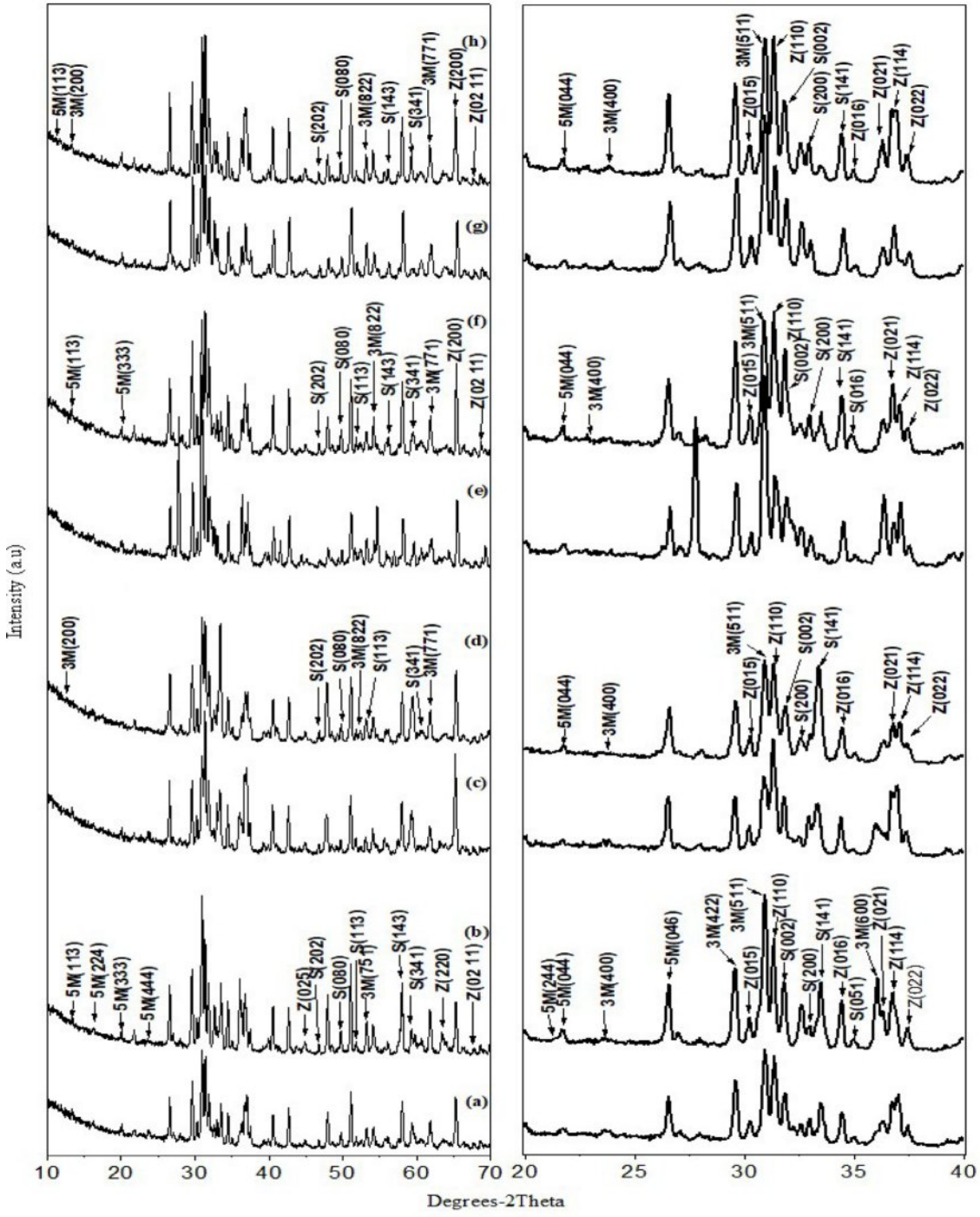

Fig. 1. Comparison of the ceramics' XRD spectra; (a) Mur before γ irradiation (b) Mur after γ irradiation, (c) Sr-Mur before γ irradiation, (d) Sr-Mur after γ irradiation (e) Cs-Mur before γ irradiation, (f) Cs-Mur after γ irradiation, (g) (Sr-Cs)-Mur before γ irradiation, (h) (Sr-Cs)-Mur after γ irradiation.

based ceramic by sintering at various temperatures between 1250-1350 °C. A.S. Pakhomova et al. [27, 28] published a calculated theoretical density of 4.568 g/cm^3 for a 3M Murataite and 4.541 g/cm^3 for a 8M Murataite, both synthesized by sintering at 1500 °C. J.W. Adams et al. [6] found a theoretical density value of 4.64 g/cm^3 and a measured Archimedes density of 4.69 g/cm^3, for a natural Murataite.

The published density values in the literature are slightly higher than those of the present study. The noted differences are mainly due to the employed measurement method (especially the Archimedes density takes into account the external porosity only) the sintering temperatures, the materials chemical compositions, which induces differences in the formed crystalline phases. All these parameters may involve differences in the reported density values.

Phases' identification

The XRD spectra of all materials, before and after irradiation for Mur, Sr-Mur, Cs-Mur, and (Sr-Cs)-Mur, respectively, are depicted on Fig. 1. The phases' identification, as well as the crystallographic parameter calculations are carried out using X'Pert High score Plus software [25]. Data on the materials phases' identification and semi-quantitative analyses are reported in Table 3. The whole of materials are polyphasic ones. The major identified phase is a 5M Murataite, noted 5M (>86%), indicating that the materials are successfully synthesized. This phase is an F-43m cubic phase with a 216-space group, identified to the JCPDS n° 98-042-2137. The secondary phases are mainly Zincohoegbomite (noted Z) (JCPDS: 98-005-4165), and a few percentages of 3M Murataite (noted 3M) (JCPDS: 01-086-0888) and Srebrodolskite (noted S) (JCPDS: 96-900-5441). Oxides reagents' traces are also identified.

Except for the reference material, for the whole of ceramics, the gamma irradiation decreases significantly the amount of 5M Murataite phase, below 80%, especially for the Cs-Mur and the (Sr,Cs)-Mur co-doped materials. One can assume that the 5M Murataite is in a certain degree of structural disorder, which affects the response to a radiation solicitation, by increasing certain hkl reflexions. Indeed, J. Lian et al. [31] have studied the ion-beam induced amorphizations in a Murataite structure and concluded that a high degree of structural disorder induces a better stability in the material compared to that of a Murataite superstructure. The doping of the material with Sr provokes the raise of Zincohoegbomite phase of $H_2Al_{15.44}Fe_{2.18}O_{32}Ti_{1.2}Zn_{3.18}$ skeleton. This is traduced by the peaks' raise in the XRD spectra' region of 2θ=20 to 40°. This suggests that Zincohoegbomite structure may accommodate Sr in Zn sites. Cs, which is a bigger atom compared with Sr is preferably hosted in 5M Murataite phase, that is why it is abundant in Cs-Mur material.

However, after gamma irradiation, the contents in Zincohoegbomite phase raises noticeably in the Cs-Mur and the (Sr, Cs)-Mur suggesting that the oxygen defects created by irradiation facilitate both Sr and Cs doping in Zincohoegbomite, that grows in the materials to the detriment of 5M Murataite phase. This phenomenon can explain why there are significant variations in the materials densities. Indeed, the phases in the Murataite bearing materials have different densities, namely the 5M Murataite theoretical density (noted TD) is about 4.97, whereas the Zincohoegbomite has a TD density of 4.23, Srebrodolskite a TD value of 4.04, and 3M Murataite a TD value of 4.05. S. V. Stefanovsky et al. [32] demonstrated the link between both the dopants' particles sizes and their valences and the affinity in doping the host phases. More clearly, the Murataite can accommodate preferably the heavy REE and tetravalent actinides rather than the light trivalent REE, which suggests that Sr will be accommodated in Zincohoegbomite rather than in 5M Murataite phase, especially after a subsequent gamma irradiation of the sintered materials.

However, one can aknowledge that the hkl reflex intensity is enhanced in the identified phases, along with the changes in the phase's contents. This phenomenon has been reported by N.P. Laverov et al. [33] which noted that the gamma radiation effects depend on the Murataite' chemical composition. Slight sifts of the peaks toward the left (<0.5°) denotes a raise of the lattice parameters induced by the particles displacements (O^{2-} and doping cations) occurring in the crystals under gamma irradiation; [34] whereas the peaks slight shifts towards the right (<0.5°) are occasioned by the diminution of the lattice parameters [11, 12, 35, 36]. Residual constraints in the crystals can also occur along with the particles displacements, those influencing the lattice parameters variations and then the peaks displacements [37].

Table 3. The materials' XRD data on phases identification and semi-quantitative analysis (in %), before and after γ-irradiation.

Material		Mur		Sr-Mur		Cs-Mur		(Sr-Cs)-Mur	
Archimedes density (g/cm^3)		3.415	3.752	3.355	3.711	3.866	3.748	3.833	3.693
Phases (%)	JCPDS	Before	After	Before	After	Before	After	Before	After
3M Murataite	01-086-0888	1	1	2	2	1	3	1	7
5M Murataite	98-042-2137	**91**	**92**	**86**	**80**	**94**	**72**	**90**	**47**
Zincohoegbomite	98-005-4165	6	5	9	10	4	19	4	37
Srebrodolskite	96-900-5441	2	2	3	7	2	6	4	9

After irradiation, the phases' main peaks intensities increase, indicating changes in the crystals' lattices. Especially, the relative intensities of 5M Murataite peaks: (333), (444), (044), (113), and the 3M Murataite major peaks: (511), (200), (400), (822), (771). The main Zincohoegbomite peaks are strong in intensity, namely: (110), (021), (015), (220), (0,2,11), (016), (022), and (114) this last overlaps the (400) peaks of 3M Murataite. The main Srebrodolskite peaks appears namely: (141) (the 100%), (113), (002), (200), (141), (202), (080), (143), (341). The (020) peak overlaps the (113) 3M Murataite peak. The peak (114) overlaps the (400) 3M Murataite peak and the (200) Srebrodolskite peak. The (-532) peak overlaps the (220) Zincohoegbomite' peak.

For the (Sr, Cs)-Mur material, the significant shift to the right (about 5°) of the whole of XRD spectrum is attributed to the torsions occurring in the crystals' lattices after the (Sr, Cs) co-doping in the material, whatever the material is gamma irradiated or no.

S.V. Stefanovsky et al. [38] synthesize a U-bearing Murataite ceramic with the following chemical composition (in wt.%) 5 Al_2O_3, 10 CaO, 55 TiO_2, 10 MnO, 5 Fe_2O_3, 5 ZrO_2, 10 UO_2, by several ways of synthesis, namely: melt of an oxide mixture either in Pt ampoules or in glassy carbon crucibles, and also in a cold crucible inductive melting furnace. The authors concluded that the synthesis method strongly affects the resulting formed phases, as there is a direct link between the created oxygen defects in the structure and the cations movements, that oriented the growth of the formed phases.

In the present study, only the Mur reference material is not affected by 10^5 Gy of Co-60, highlighting the fact that both Cs and (Sr, Cs) doping has altered the Murataite phase after irradiation. S.V. Yudintsev et al. [39] have irradiated a Murataite bearing material reach in crichtonite, synthesized in a cold crucible. The crichtonite is amorphized whereas the Murataite is not altered by gamma irradiation, with a dose of 22 10^6 Gy. It is important to note that M.V. Skvortsov et al [40] have irradiated lanthanides (La, Ce, Ho) bearing Murataite based materials at a dose 2.2 10^7 Gy of Co-60. They report that this gamma dose didn't affect the crystalline structure of the materials.

The average crystallite size (D) was calculated using Debye-Scherer formula. The values are within the range 401 Å - 533 Å before γ-irradiation and about 320 Å - 457 Å after γ-irradiation (Table 4). We note a slight drop in the size of the crystallites after irradiation revealing that both Cs and Sr doping are slightly affecting the 5M Murataite lattice size. This support the preceding results which show that Cs and Sr are preferably hosted in Zincohoegbomite phase.

Table 4. Comparison between the 5M Murataite crystallite size before and after irradiation.

	D (Å) Before γ-irradiation	D (Å) After γ-irradiation
Mur	401 ± 1	320 ± 1
Sr-Mur	533 ± 2	457 ± 1
Cs-Mur	400 ± 1	356 ± 1
(Sr-Cs)-Mur	457 ± 1	457 ± 1

The materials SEM observations

For the whole of Murataite materials, the SEM micrographs are depicted on Fig. 2. The SEM images analysis gives the main differences in materials microstructural features before and after irradiations. On the pictures, the main crystallites are associated with 5M Murataite phase. The minor grains of hexagonal and orthorhombic crystals shapes are associated to Zincohoegbomite and Srebrodolskite phases, respectively. These last two phases clearly growth from the grains' boundaries.

This results in phases' growth on the surface of the grains piles, for Zincohoegbomite and Srebrodolskite after irradiation. The microporosity doesn't decreases for the reference material and the Sr-doped material, thus giving a coherent and tight structure. The homogeneity in the phase distribution is preserved. And the murataites' crystallites sizes are comparable before and after irradiation.

A certain microporosity seems to appear for the Cs and Cs-Sr doped materials. The aggregates of different sizes, clearly observed before irradiation (Fig. 3), are altered after irradiation, especially on pictures of low magnification, revealing that both phases' changes and movements are driven by ions (Cs and Sr) migrations (O^{2-} and then cations displacements) under gamma irradiation.

For the whole of materials, and for the chosen irradiation dose, coherent arrangements of phases are observed after irradiation, and the heterogeneities observed (especially in the reference material and Sr-Mur material) in the crystallite's arrangements disappear.

The internal micro-porosity on the pictures is directly linked to the materials densities which are lower than those usually found in the literature (Table 2), especially for Cs-Mur and (Sr-Cs)-Mur materials.

As calculated using Debye–Scherer formula, the 5M Murataite grains size on the pictures tends to diminish after irradiation.

The global conclusion that can be made is that irradiation does not favour the 5M Murataite growth except for the reference material, the global microstructure appearance is preserved for the whole.

S.V. Yudintsev et al. [40] have demonstrated that the heterogeneity of Murataite grains is frequently observed in Murataite-based ceramics, with 8M Murataite and 5M Murataite coherently intercalated with pyrochlore phase.

Materials Vickers microhardness' measurements

For the whole of materials, Vickers microhardness measurements are mean values of 10 consecutive

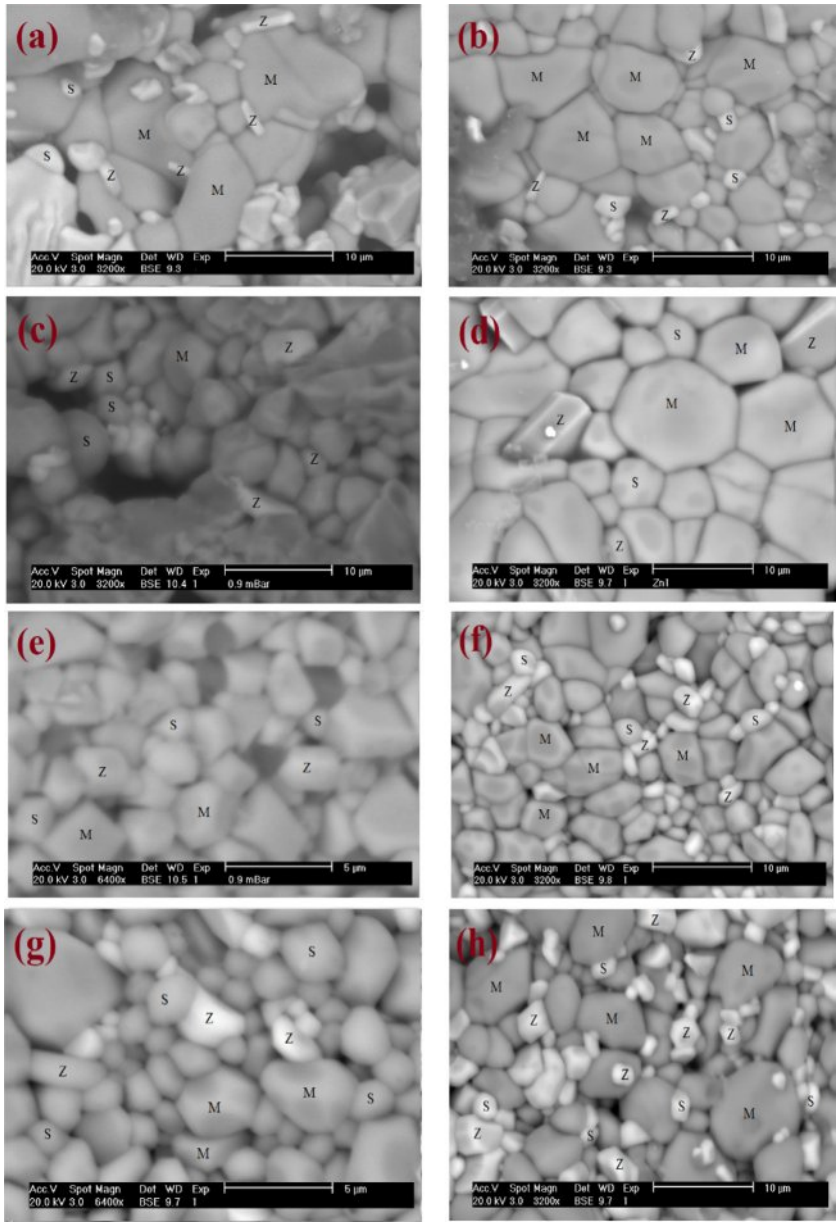

Fig. 2. Comparison of the ceramics' SEM micrographs before and after irradiation. (a) Mur ceramic before γ irradiation, (b) Mur ceramic after γ irradiation, (c) (Sr-Mur) before γ irradiation, (d) (Sr-Mur) after γ irradiation, (e) (Cs-Mur) before γ irradiation, (f) (Cs-Mur) after γ irradiation, (g) (Sr-Cs)-Mur before γ irradiation, and (h) (Sr-Cs)-Mur after γ irradiation.

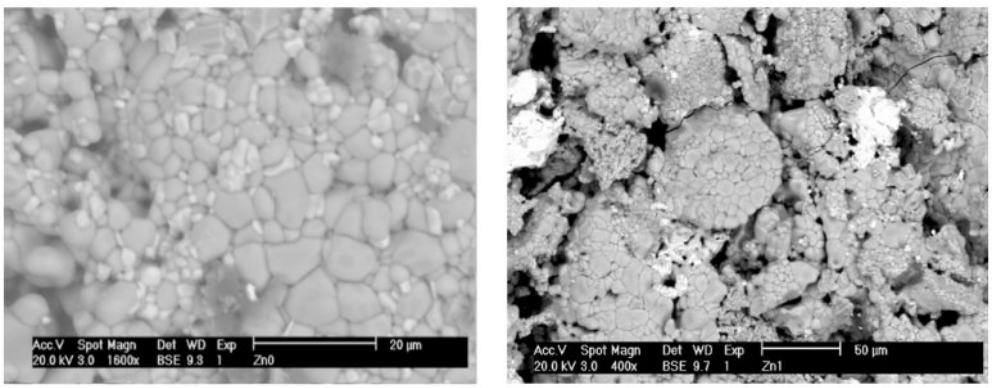

Fig. 3. Typical grains aggregates in Murataite materials at 400x and 1600x before γ irradiation.

Table 5. Comparison between the microhardnesses of the synthesized Murataites before and after γ irradiation.

Material	Mur		Sr-Mur		Cs-Mur		(Sr-Cs)-Mur	
Archimedes density (g/cm^3)	3.415	3.752	3.355	3.711	3.866	3.748	3.833	3.693
Microhardnesse (HV_{force})	523 HV_1	516 $HV_{0.2}$	646 $HV_{0.5}$	470 HV_2	417 $HV_{0.5}$	410 $HV_{0.5}$	607 $HV_{0.5}$	607 $HV_{0.5}$
Phase	Phases (%)							
	Before	After	Before	After	Before	After	Before	After
3M Murataite	1	1	2	2	1	3	1	7
5M Murataite	91	92	86	80	94	72	90	47
Zincohoegbomite	6	5	9	10	4	19	4	37
Srebrodolskite	2	2	3	7	2	6	4	9

measures, which lead to the results given in Table 5. The lowercase index indicates the loaded charge applied during the measurements in Kg.

The Cs-Mur material has the lower Vickers microhardness compared with the other studied materials. Except for the Sr-Mur material, for which the gamma irradiation lowers significantly the Vickers microhardness values, the gamma irradiation has no significant impact on the material' microhardness. The decrease of microhardness in Sr-Mur has no relation with the Murataite-5 phases' content, which is quite similar with the other studied materials. This can be linked with the other microstructural features as the SEM observations and the global porosity and density of the materials.

In general, except for Cs-Mur material, the microhardness values are strong values, all over 500 HV, and are suitable for a ceramic dedicated for radioactive waste confinement. There are scarce studies reporting the Vickers microhardeness of such minerals. J.W. Adams et al. [6] describe a natural mineral of Murataite, derived from the alkalic Mount Rosa Granite, and measure a very high microhardness about 827 HV (a range of 782-870 HV determined at 15 indentations made at l00 g load). This strong hardness is due to its natural origin, and shows a coherent natural crystal genesis in the bulk of the material. Some complex related structures as Nöggerathite-(Ce), $(Ce,Ca)_2Zr_2(Nb,Ti)(Ti,Nb)_2Fe^{2+}O_{14}$, has a comparable microhardness value (615 HV) [41].

Conclusions

A polysomatic Murataite structure with the chemical formula: 10% ZnO, 12% CaO, 7% Er_2O_3, 53% TiO_2, 7% ZrO_2, 6% Fe_2O_3, 5% Al_2O_3, was synthesized by sintering in air at 1250 °C for 10 h. Four chemical compositions were obtained by doping the material with Sr, Cs and both Sr and Cs elements. These last represent alkaline and alkaline earth elements, often present in mixtures of radioactive wastes. The effect of irradiation on the microstructure of the materials was examined for a total γ dose of 10^5 Gy, with a dose rate of 10.75 Gy/min.

In these conditions, the γ-radiation has a significant effect on the ceramics' Archimedes density, which increases slightly in the Mur reference material and by doping Murataite with Sr (Sr-Mur), contrary to the Cs-Mur and Sr-Cs-Mur ceramics, for which the irradiation raised the materials porosity, affecting the materials density.

For the whole of materials, the main identified phase is a 5M Murataite (>86%), with an F-43m cubic symmetry and a 216 space group. The secondary phases are Zincohoegbomite, Srebrodolskite and 3M Murataite.

The doping of the material with Sr provokes the raise of Zincohoegbomite phase to the detriment of 5M Murataite. This suggests that Zincohoegbomite structure may accommodate Sr in Zn sites. Cs is preferably hosted in 5M Murataite phase, before irradiation. After irradiation, Sr is easily hosted in Zincohoegbomite rather than in 5M Murataite phase.

In general, only the Mur reference material is not affected by 10^5 Gy of Co-60 radiations, highlighting the fact that Cs doping and (Sr, Cs) doping has altered the 5M Murataite phase content after irradiation, but not the 5M Murataite crystallites despite variation in the lattice parameter, which is significant for the co-doped (Sr,Cs)-Mur material.

The SEM pictures depict the main crystallites associated to 5M Murataite phase. The minor grains of hexagonal and orthorhombic crystals shapes are associated to Zincohoegbomite and Srebrodolskite phases, respectively. The aggregates of different sizes observed before irradiation are altered after irradiation.

The global conclusion is that γ irradiation has a positive impact on the Mur reference material as well as on the Sr-Mur material. However it does not favour the 5M Murataite growth, when doping the material with Cs and both Sr-Cs.

With regard to the 5M Murataite phase content, both the reference material and Sr-Mur material composition are the optimum chemical composition and give the optimum murataites' phase content after irradiation, as well as suitable density values and good mechanical properties, being in mind that the vickers microhardenesses are all strong values (over 400HV) and are not affected by gamma irradiation.

Further investigations should be undertaken with

varying the γ irradiation dose in a larger interval to make conclusions valuable on the real effect of γ irradiations on such a polysomatic structure.

References

1. R. Souag, N. Kamel, M. Hammadi, Z. Kamel, D. Moudir, F. Aouchiche, and S. Kamariz, J. Ceram. Process. Res. 16[1] (2015) 150-155.
2. V.S. Urusov, N.I. Organova, O.V. Karimova, S.V. Yudintsev, and R.C. Ewing, Crystallogr. Rep. 52[1] (2007) 37-46.
3. S.V. Stefanovsky, S.V. Yudintsev, M.S. Nickolsky, O.I. Stefanovsky, and M.V. Skvortsov, J. Nucl. Mater. 529 (2020) 151958.
4. K.I. Maslakov, Y.A. Teterin, O.I. Stefanovskaya, S.N. Kalmykov, A.Y. Teterin, K.E. Ivanov, S.S. Danilov, and B.F. Myasoedov, Radiochemistry. 63[6] (2021) 801-810.
5. S.V. Stefanovsky, S.V. Yudintsev, S.E. Vinokurov, and B.F. Myasoedov, Geochem. Int. 54[13] (2016) 1136-1156.
6. J.W. Adams, T. Botinelly, W.N. Sharp, and K. Robinson, Am. Min. 59 (1974) 172-176.
7. R.S.S. Maki, P.E.D. Morgan, and Y. Suzuki, J. Alloys Compd. 698 (2017) 99-102.
8. B.I. Omel'yanenko, and B.S. Nikonov, Dokl. Earth Sci. 363[8] (1998) 1104-1106.
9. S. Perevalov, S.V. Stefanovsky, S.V. Yudintsev, A.V. Mokhov, and A.G. Ptashkin, Radiochim Acta. 94[9-11] (2006) 509-514.
10. S.V. Yudintsev, S.V. Stefanovsky, B.S. Nikonov, O.I. Stefanovsky, M.S. Nickolsky, and M.V. Skvortsov. J. Nucl. Mater. 517 (2019) 371-379.
11. B.J. Park, J.E. Lim, J.S. Yuk, S.H. Lee, M.G. Lee, J.S. Park, and S.G. Lee, J. Ceram. Process. Res. 25[1] (2024) 48-55.
12. M.M. Eltabey, I.A. Ali, H.E. Hassan, and M.N.H. Comsan, J. Mater. Sci. 46 (2011) 2294-2299.
13. O.M. Hemeda and M. El-Saadawy, J. Mag. Mag. Mater, 256 (2003) 63-68.
14. V.J. Angadi, A.V. Anupama, R. Kumar, H.M. Somashekarappa, K. Praveena, B. Rudraswamy, and B. Sahoo, Ceram. Int. [14] (2016) 15933-15939.
15. M.K. Gatasheh, M.S. Alkathy, H.A. Kassim, J.P. Goud, and J.A. Eiras, Open Chem. 21[1] (2023) 20230117.
16. G.P. Pells, J. Nucl. Mater. 155 (1988) 67-76.
17. D.P. Kiryuhin, I.P. Kim, V.M. Buznik, L.N. Ignat'eva, V.G. Kuryavyi, and S.G. Sakharov, Russ. J. Gen. Chem. 79[3] (2009) 589-595.
18. Y. Chen, Q. Zhang, F. Peng, W. Liu, D. Sun, R. Dou, H. Zhang, Y. He, S. Han, and S. Yin, J. Lumin. 205 (2019) 109-114.
19. R.A. Perez-Herrera, A. Stancalie, P. Cabezudo, D. Sporea, D. Neguţ, and M. Lopez-Amo, Sensors. 20[11] (2020) 3017.
20. S.H. Mahmud, S.C. Das, M.Z.I. Mollah, M.M. Ul-Hoque, K.S. Al-Mugren, M.R.I. Faruque, and R.A. Khan, J. Mater. Res. Technol. 26 (2023) 6623-6635.
21. A.A. Lizin, S.V. Tomilin, S.S. Poglyad, E.A. Pryzhevskaya, S.V. Yudintsev, and S.V. Stefanovsky, J. Radioanal. Nucl. Chem. 318[3] (2018) 2363-2372.
22. A.V. Samoryadov, V.B. Ivanov, and E.V. Kalugina, Russian Journal of General Chemistry. 64[4] (2020) 3-19.
23. C.W. Bock, A.K. Katz, G.D. Markham, and J.P. Glusker, J. Am. Chem. Soc. 121 (1999) 7360-7372.
24. R.D. Shannon, Acta Cryst. 32[5] (1976) 751-767.
25. Philips X'Pert High Score Plus Database Package, International Center for Diffraction Data, Newtown Square, PA, 2011.
26. M.P. Bradley, J.V. Porto, S. Rainville, J.K. Thompson, and D.E. Pritchard, Phys. Rev. Lett. 83[22] (1999) 4510-4513.
27. A.N. Lukinykh, S.V. Tomilin, A.A. Lizin, S.V. Yudintsev, and S.V. Stefanovskii, Radiochemistry. 50[5] (2008) 541-546.
28. A.S. Pakhomova, S.V. Krivovichev, S.V. Yudintsev, and S.V. Stefanovsky, Z. Kristallogr. 223[3] (2013) 151-156.
29. A.S. Pakhomova, S.V. Krivovichev, S.V. Yudintsev, and S.V. Stefanovsky, Eur. J. Mineral. 28[1] (2016) 205-214.
30. S.V. Krivovichev, V.S. Urusov, S.V. Yudintsev, S.V. Stefanovsky, O.V. Karimova, and N.N. Organova, Minerals as advanced materials II. (2012) 293-304.
31. J. Lian, L.M. Wang, R.C. Ewing, S.V. Yudintsev, and S.V. Stefanovsky, J. Appl. Phys. 97[11] (2005) 113536.
32. S.V. Stefanovsky, A.G. Ptashkin, O.A. Knyazev, M.S. Zen'kovskaya, and O.I. Stefanovsky, WM 2008 Conference, Feb. 24-28, Abstract N° 8036, 2008.
33. N.P. Laverov, S.V. Yudintsev, T.S. Yudintseva, S.V. Stefanovsky, R.C. Ewing, J. Lian, S. Utsunomiya, and L.M. Wang, Geology of Ore Deposits. 45[6] (2003) 423-451.
34. S. Chelbi, L. Hammiche, D. Djouadi, and A. Chelouche, Rev. Algér. Phys. 2[2] (2015) 69-73.
35. I.S. Kondrashkova, K.D. Martinson, N.V. Zakharova, and V.I. Popkov, Russ. J. Gen. Chem. 88[12] (2018) 2465-2471.
36. M.A. Ahmed, E. Ateia, G. Abdelatif, and F.M. Salem, Mater. Chem. Phys. 81 (2003) 63-77.
37. V.M. Kaganer, R. Köhler, M. Schmidbauer, and R. Opitz, and B. Jenichen, Phys. Rev. B. 55[3] (1997) 1793.
38. S.V. Stefanovsky, A.G. Ptashkin, O.A. Knyazev, S.V. Yudintsev, B.S. Nikonov, and O.I. Stefanovsky, Ceram. Int. 44 (2018) 9773-9779.
39. S.V. Yudintsev, O.I. Stefanovskaya, M.S. Nikolsky, M.V. Skvortsov, and B.S. Nikonov, Dokl. Earth Sci. 498[1] (2021) 444-449.
40. S.V. Yudintsev, M.S. Nickolsky, M.I. Ojovan, O.I. Stefanovsky, B.S. Nikonov, and A.S. Ulanova, Minerals. 15[17] (2022) 6091.
41. N.V. Chukanov, N.V. Zubkova, S.N. Britvin, I.V. Pekov, M.F. Vigasina, C. Schäfer, B. Ternes, W. Schüller, Y.S. Polekhovsky, V.N. Ermolaeva, and D.Y. Pushcharovsky, Minerals. 8[10] (2018) 449.